Next-to-leading-order predictions for single vector-like quark production at the LHC

Giacomo Cacciapaglia [a], Alexandra Carvalho [b], Aldo Deandrea [a], Thomas Flacke [c,*], Benjamin Fuks [d,e], Devdatta Majumder [f], Luca Panizzi [g,h], Hua-Sheng Shao [d]

[a] *Univ Lyon, Université Lyon 1, CNRS/IN2P3, IPNL, 69622 Villeurbanne, France*
[b] *NICPB, Akadeemia tee, Tallinn, Estonia*
[c] *Center for Theoretical Physics of the Universe, Institute for Basic Science (IBS), Daejeon 34126, Republic of Korea*
[d] *Laboratoire de Physique Théorique et Hautes Energies (LPTHE), UMR 7589, Sorbonne Université et CNRS, 4 place Jussieu, 75252 Paris Cedex 05, France*
[e] *Institut Universitaire de France, 103 boulevard Saint-Michel, 75005 Paris, France*
[f] *The University of Kansas, Lawrence, USA*
[g] *Department of Physics and Astronomy, Uppsala University, Box 516, SE-751 20 Uppsala, Sweden*
[h] *School of Physics and Astronomy, University of Southampton, Highfield, Southampton SO17 1BJ, UK*

ARTICLE INFO

ABSTRACT

We propose simulation strategies for single production of third generation vector-like quarks at the LHC, implementing next-to-leading-order corrections in QCD and studying in detail their effect on cross sections and differential distributions. We also investigate the differences and the relative incertitudes induced by the use of the Four-Flavour Number Scheme *versus* the Five-Flavour Number Scheme. As a phenomenological illustration, we concentrate on the production of vector-like quarks coupling to the third generation of the Standard Model in association with a jet and assuming standard couplings to gauge and Higgs bosons.

1. Introduction

Many extensions of the Standard Model feature vector-like quarks, or quarks whose left-handed and right-handed components lie in the same representation of the Standard Model gauge symmetry group. Their existence is predicted, for instance, in models featuring extra dimensions, an extended gauge symmetry or a composite Higgs sector [1–5], and their expected mass scale is generally such that they could be observed in current and future LHC data. For this reason, vector-like quark searches play a major role in the ATLAS and CMS searches for new phenomena. Current searches mostly rely on signatures induced by both their pair and single production, although present bounds are mostly driven by the strong pair production mechanism, followed by a decay pattern in which each vector-like quark is assumed to decay into a Standard Model gauge or Higgs boson and a third-generation quark,

both legs being potentially decaying differently. Taking into account an integrated luminosity of 35–36 fb^{-1}, vector-like quarks of about 1.2 TeV are conservatively excluded, regardless of the decay details [6–10], although such a bound can in principle be lowered when exotic decay modes into non-standard particles exist [11] or if they decay into lighter Standard Model quark generations.

Vector-like quark decays are driven by interactions that also induce their single (weak) production in hadronic collisions. Although the exact details of the corresponding production mechanism are model-dependent, single production becomes more and more relevant with respect to pair production once the mass of the extra quarks is large enough, by virtue of a smaller phase-space suppression [12–14]. Whilst the corresponding backgrounds are usually large, they can be controlled to a large extent by making use of the properties of the jets accompanying the singly-produced heavy quark. The leading jet tends to be forward and can thus be an efficient handle for background rejection, as illustrated by recent experimental searches [15–19]. All those searches, however, rely on simulations of the signal at the leading-order (LO) accuracy in QCD, although next-to-leading-order (NLO) corrections are expected to substantially impact the predictions [20,21].

In this work, we study the single production of a vector-like top partner and investigate the effects of NLO corrections on both the

* Corresponding author.
E-mail addresses: g.cacciapaglia@ipnl.in2p3.fr (G. Cacciapaglia), alexandra.oliveira@cern.ch (A. Carvalho), deandrea@ipnl.in2p3.fr (A. Deandrea), flacke@ibs.re.kr (T. Flacke), fuks@lpthe.jussieu.fr (B. Fuks), Devdatta.Majumder@cern.ch (D. Majumder), luca.panizzi@physics.uu.se (L. Panizzi), hshao@lpthe.jussieu.fr (H.-S. Shao).
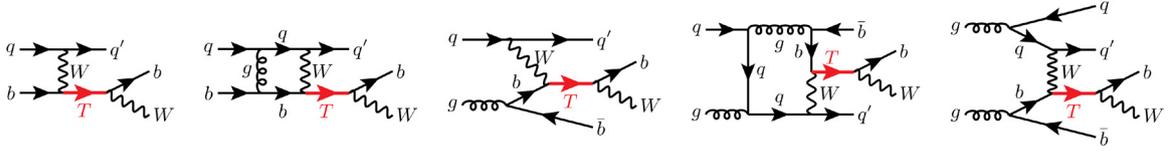
Fig. 1. Representative Feynman diagrams for single vector-like T-quark production. We show typical tree-level (leftmost), virtual loop (second leftmost) and real emission (centre) contributions in the 5FNS, the latter contributing also at the tree-level in the 4FNS. Typical 4FNS loop contributions and real emission diagrams are respectively presented in the second rightmost and rightmost figures.

total rates and differential distributions. We carefully assess the reduction of the theoretical uncertainties originating from the inclusion of higher-order contributions, and consider two options for the number of active quark flavors in the proton, namely four and five. In the former case, the bottom quark is massive and the associated parton density is taken vanishing. In the latter case, the bottom quark is massless and all bottom-quark mass effects are effectively resummed into a bottom parton density. We detail the consequences of such a choice on the total production rate, as well as on several exclusive kinematic observables, such as the final-state jet properties, that play a big role in the search strategies at the LHC in terms of selection cuts, efficiencies and background *versus* signal discrimination.

The rest of this work is organized as follows. In Section 2, we describe the vector-like quark simplified model that we have adopted for our study, and provide information on our framework for the precise calculation of physical observables. Section 3 includes our results and main features of the study. We give our conclusions in Section 4.

2. Theoretical framework and technical details

In order to investigate the phenomenology associated with the single production of a vector-like top partner, we consider a simplified model in which the Standard Model field content is extended by four species of extra quarks X, T, B and Y respectively of electric charges 5/3, 2/3, −1/3 and −4/3. Focusing on third generation partners, the additional heavy quarks solely couple with the Standard Model top and bottom quarks, t and b, and we forbid any mixing of the new states with Standard Model lighter quarks. The corresponding Lagrangian, invariant under $SU(3)_c \times U(1)_Q$ transformations, is then given by [21]

$$\mathcal{L} = \sum_{Q=X,T,B,Y} \left[i\bar{Q}\slashed{D}Q - M_Q\,\bar{Q}\,Q \right]$$
$$- \sum_{Q=T,B} \left[h\bar{Q}\left(\hat{\kappa}_L^Q P_L + \hat{\kappa}_R^Q P_R\right)q + \text{h.c.} \right]$$
$$+ \frac{g}{2c_W} \sum_{Q=T,B} \left[\bar{Q}\slashed{Z}\left(\tilde{\kappa}_L^Q P_L + \tilde{\kappa}_R^Q P_R\right)q + \text{h.c.} \right] \quad (2.1)$$
$$+ \frac{g}{\sqrt{2}} \sum_{Q=X,T,B,Y} \left[\bar{Q}\slashed{W}\left(\kappa_L^Q P_L + \kappa_R^Q P_R\right)q + \text{h.c.} \right],$$

where all the electroweak couplings κ, $\tilde{\kappa}$ and $\hat{\kappa}$ are considered as free parameters. In the Lagrangian above, q stands for b (t) for the neutral-current interactions of the B (T) quark and for the charged-current interactions of the Y and T (X and B) quarks, while Z, W are the weak gauge bosons and h is the Higgs boson. The covariant derivatives include both QCD and QED interactions, while the weak-boson couplings to a pair of vector-like quarks are omitted as model dependent, usually small and not relevant for the present study [22]. Moreover, c_W stands for the cosine of the electroweak mixing angle.

We consider the production, at the LHC, of a single vector-like quark and aim to assess the impact of NLO corrections in QCD on the predictions. To this aim, we make use of the existing implementation [21] of the Lagrangian of Eq. (2.1) into FeynRules [23], which allows for the generation of an NLO UFO model [24] through a joint usage of FeynRules, NLOCT [25] and FeynArts [26]. This UFO model contains, in addition to tree-level model information, ultraviolet counterterms as well as rational R_2 Feynman rules [27] so that it can be used within MG5_aMC@NLO [28] for NLO calculations in QCD. The cancellation of the ultraviolet divergences appearing in the virtual one-loop amplitudes is ensured by the presence of the counter-terms in the UFO, and the finite part of the loop-integrals is evaluated numerically in four dimensions, the model-dependent and process-dependent parts of the rational terms being extracted from the R_2 information included in the UFO.

Predictions are achieved by convoluting LO and NLO matrix elements with the NNPDF 3.1 set of parton densities [29] accessed via the LHAPDF 6 library [30]. After making use of MadSpin [31] to model the extra quark decays at LO, we match the fixed-order results with the parton shower algorithm of the Pythia 8 package [32], which we also use, within the MG5_aMC@NLO package, to simulate the hadronisation process of all final-state coloured partons. Event reconstruction is performed with MadAnalysis 5 [33,34], through which we use the anti-k_T algorithm [35] with a radius parameter set to $R = 0.4$ as implemented in FastJet [36].

3. Single VLQ production at the LHC

In this section, we investigate the phenomenology associated with the single production of a vector-like quark at the LHC, in proton-proton collisions at a centre-of-mass energy of 13 TeV. We study the impact of the NLO corrections both at the level of the total rate and for differential cross sections. For the latter, we put the emphasis on observables crucial for providing handles on the discrimination of a potential signal from the background, such as the properties of the jets produced together with the heavy quark.

We consider the production of vector-like quarks interacting with the Standard Model third-generation quarks, so that the associated single-production processes involve bottom quarks, as shown in Fig. 1. The bottom quarks can be accounted for in the calculations in two different ways. In the so-called four-flavour-number scheme (4FNS), bottom quarks, which are significantly heavier than the proton, are treated as heavy flavours. Thus, they cannot contribute to the proton wave-function and are solely produced as massive final-state particles. In the five-flavour-number scheme (5FNS), the mass of the bottom quark is neglected with respect to the hard scale of the processes under consideration, and its effects are resummed into a bottom quark density in the proton that is not present in the 4FNS. Whilst at all orders in perturbation theory the two schemes are identical, the way in which the perturbative expansion is organised is different at a given finite order, so that predictions may not necessarily match. In this work, we assess the implications on the single production of a vector-

Table 1

LO and NLO QCD inclusive cross sections for the single production of a heavy T-quark in the 4FNS and 5FNS, in the context of LHC collisions at a centre-of-mass energy $\sqrt{s} = 13$ TeV. The results are shown together with the associated scale and parton density uncertainties.

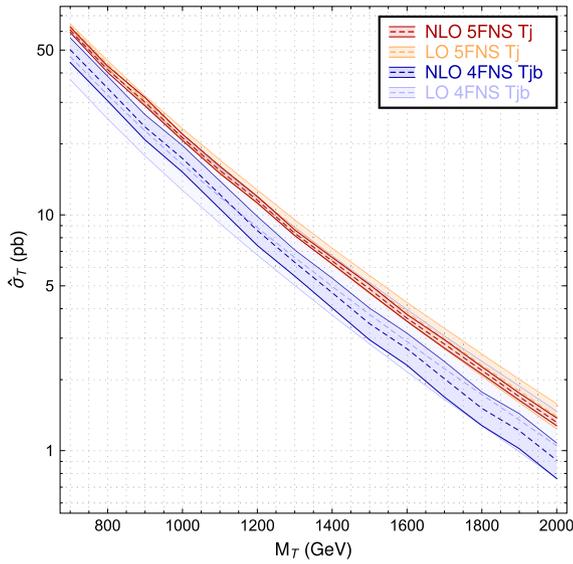| M_T [GeV]	$\hat{\sigma}_{LO}^{4FNS}$ [pb]	$\hat{\sigma}_{NLO}^{4FNS}$ [pb]	$\hat{\sigma}_{LO}^{5FNS}$ [pb]	$\hat{\sigma}_{NLO}^{5FNS}$ [pb]
800	$32.28^{+27.8\%+0.7\%}_{-20.0\%-0.7\%}$	$34.49^{+10.9\%+1.4\%}_{-10.2\%-1.4\%}$	$43.75^{+2.1\%+1.0\%}_{-2.7\%-1.0\%}$	$41.32^{+2.4\%+1.2\%}_{-1.4\%-1.2\%}$
1200	$8.83^{+32.1\%+1.3\%}_{-22.2\%-1.3\%}$	$8.59^{+12.8\%+1.9\%}_{-11.7\%-1.9\%}$	$11.93^{+5.6\%+1.2\%}_{-5.4\%-1.2\%}$	$11.55^{+2.2\%+1.6\%}_{-1.0\%-1.6\%}$
1600	$2.90^{+35.4\%+1.5\%}_{-24.0\%-1.5\%}$	$2.71^{+13.9\%+2.4\%}_{-12.5\%-2.4\%}$	$3.87^{+8.2\%+1.7\%}_{-7.3\%-1.7\%}$	$3.65^{+1.9\%+1.9\%}_{-1.0\%-1.9\%}$
2000	$1.05^{+38.2\%+1.9\%}_{-25.3\%-1.9\%}$	$0.91^{+15.5\%+2.8\%}_{-13.6\%-2.8\%}$	$1.40^{+10.4\%+2.7\%}_{-8.9\%-2.7\%}$	$1.32^{+1.9\%+2.5\%}_{-0.8\%-2.5\%}$

Fig. 2. Total production cross section for single T-quark production at the LHC. We present results at the leading order in the 5FNS (orange) and 4FNS (light blue) as well as at the NLO QCD in the 5FNS (red) and in the 4FNS (dark blue). Scale and parton density 1σ uncertainties are included in the error bands.

like quark of the third generation whose dynamics stems from the Lagrangian of Eq. (2.1).

As a benchmark, we consider an up-type vector-like quark T that couples only to the W-boson. For simplicity, only the left-handed couplings have been set to non-zero values, i.e. $\kappa_L^T \neq 0$ and $\kappa_R^T = 0$. This choice is motivated by the fact that, in the case of the presence of a single vector-like quark Q, only one of the two mixing angles is large, the other being suppressed by a factor of m_q/M_Q where m_Q and m_q are the heavy quark and relevant Standard Model quark masses respectively [37]. All our results are given after factorising the whole $\frac{g}{\sqrt{2}}\kappa_L^T$ parameter, such that the total production cross-section σ_T is equal to $(\frac{g}{\sqrt{2}}\kappa_L^T)^2 \hat{\sigma}_T$.

In the 5FNS, single T-quark production originates from a $2 \to 2$ process where the heavy quark is produced in association with a jet that is mainly forward, as illustrated in the leftmost diagram of Fig. 1. The T-decay into a Wb system, i.e. the only allowed decay for the considered scenario, is also shown. Typical loop and real emission contributions are presented in the second and third diagram of the same figure. In the 4FNS, there is no b-quark density in the proton so that, at the lowest order, the heavy quark can only be produced after the splitting of a gluon into a bottom–anti-bottom pair, as illustrated by the third diagram of Fig. 1. NLO contributions to this process are illustrated by the fourth (virtual loop) and fifth (real emission) diagrams of the figure. Whilst some diagrams are common to both schemes, we recall that the mass of the bottom quark is neglected in the 5FNS whilst kept non-vanishing in the 4FNS, on top of the presence of a bottom density in the 5FNS.

In Fig. 2 and Table 1, we present LO and NLO cross section values for the single production of a vector-like T-quark, both in the 4FNS and 5FNS, and illustrate the dependence of the results on the vector-like quark mass M_T. The results are presented together with their scale uncertainties, evaluated by independently varying the renormalisation and factorisation scales by a factor of 2 up and down relatively to a central scale set to half the scalar sum of the transverse momenta of all final state particles, as well as with their parton density uncertainties extracted following the recommendations of Ref. [38]. Whilst LO parton densities should in principle be used when a convolution with LO matrix elements is in order, we have instead made use of the NLO NNPDF 3.1 set in all calculations due to the poor quality of the LO fit [29]. In the figure, the two contributions to the total error are added linearly, whereas we show them separately in the table.

In the 4FNS, NLO corrections increase the central value of the cross section by about 10% in the low-mass region, whilst reducing it by about 10% in the higher mass regime, the NLO-to-LO cross section ratio being about 1 for a heavy quark mass of about 1.1 TeV. In contrast, in the 5FNS, NLO effects always affect the cross section by reducing it by about 10%, regardless of the actual M_T value. This reduction of the cross section is connected to the virtual amplitudes appearing at NLO and contributing significantly. These channels are illustrated by the second diagram of Fig. 1 (in the 5FNS) and the fourth diagram of Fig. 1 (in the 4FNS).

Whilst results in the two schemes largely differ at LO, the compatibility between the predictions is expected to improve when higher orders are included. In the small mass regime, the compatibility between the 4FNS and 5FNS perturbative expansions is indeed improved at NLO, the differences between the total rates being of about 20% (to be compared with a 30% difference at LO). However, for heavy quark masses M_T larger than 1.1 TeV, this is not the case anymore and the difference between the two schemes stays constant at about 30%, both at LO and NLO. This is due to the fact that, whilst finite bottom mass power corrections of the type $(m_b^2/Q^2)^n$ are suppressed and negligible for the considered high scale Q, logarithms $\log Q^2/m_b^2$ could be large and may impact the two considered perturbative expansions. In this case, higher-order corrections, or the all-order resummation included in the 5FNS, could be necessary to get cross section estimates that agree better with each other [39]. Differences between the results obtained in the 4FNS and 5FNS persist at NLO for vector-like quarks with mass above about 1 TeV, so that this corresponds to a parameter space region in which large logarithms of the bottom quark mass play a significant role. In contrast, the results are perturbatively well-behaved in the light T-quark case, and a substantial agreement can be found between the predictions in both schemes. Finally, a significant reduction of the scale uncertainties is obtained in both schemes at NLO, the improvement reaching up to 50% compared with the respective LO results. Total rates however genuinely feature smaller uncertainties in the 5FNS, as stemming from the resummation of the logarithms in the bottom quark mass. As predictions matching both schemes consistently are not available, the
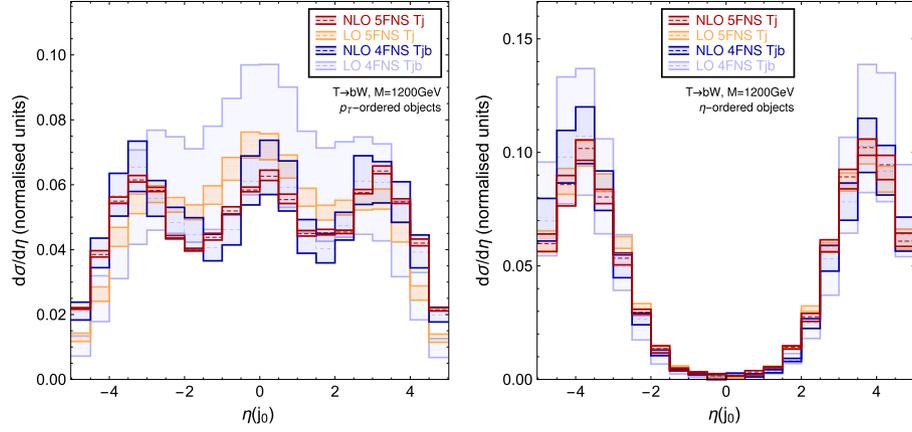
Fig. 3. Normalised distributions in the pseudorapidity of the leading non-b-jet, when the jets are ordered by transverse momentum (left) and absolute value of pseudorapidity (right). Results are given both at the LO and NLO accuracy and for the 4FNS and 5FNS, adding linearly scale and parton density uncertainties in the error bands.
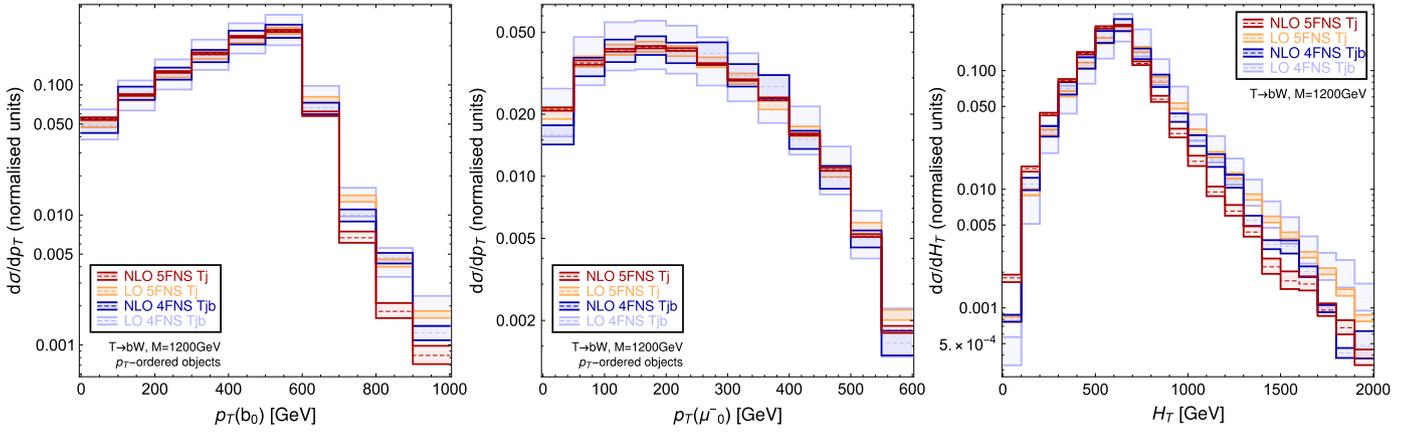

Fig. 4. Normalised distributions in the transverse momentum of the leading b-jet (left) and of the leading muon (centre) both for p_T-ordered objects, as well as in the H_T variable representing the hadronic activity (right). We present results both at the LO and NLO accuracy and for the 4FNS and 5FNS, adding linearly scale and parton density uncertainties in the error bands.

5FNS total cross section results seem preferable due to the smaller associated uncertainties and more stable K-factor (defined as the ratio of the NLO to LO predictions) with respect to M_T variations.

In the following, we asses the impact of the NLO corrections in both schemes by considering more exclusive observables, like those related to the final-state jet properties. We shall focus on the kinematics of the accompanying light jet produced in association with the vector-like quark, as well as on the b-jet originating from the vector-like-quark decay. As a benchmark, we fix the heavy quark mass to $M_T = 1.2$ TeV, a value close to the average current exclusion bounds [6–10]. We recall that, since the only non-vanishing new physics coupling in Eq. (2.1) is κ_L^T, the heavy quark T can only decay into a W-boson and a b-jet. We moreover enforce the W-boson to decay muonically for simplicity.

In Fig. 3, we present the pseudorapidity (η) distributions of the leading non-b-jet j_0, *i.e.* the leading jet for which there is no B-hadron lying in a cone of radius $R = 0.4$ centred on the direction of the jet. We show the distributions in two cases, first when the objects are ordered according to their transverse momentum p_T (left panel) and second when they are ordered according to the absolute value of their pseudorapidity (right panel). As already mentioned, this jet is of particular importance for the searches for vector-like-quark single production, as it is preferably produced in the forward direction by virtue of the t-channel production mode of a single massive particle. This forward character is indeed crucially used by the experimental searches as a handle for unravelling the signal from the background for which the corre-

sponding events feature more central jets [40]. As shown on the left panel of the figure, the hardest jet (in transverse momentum) is indeed mostly forward, the distribution featuring local maxima around $|\eta| \sim 3$, and this hardest jet is often the most forward one as demonstrated by the results in the right panel of the figure. Moreover, the inclusion of the NLO contributions is crucial to get the theoretical uncertainties under good control, as the LO predictions are plagued by uncertainties larger than 30%, a fact that can be seen as a loss of predictive power. Focusing on the NLO results, 4FNS (dark blue) and 5FNS (dark red) predictions reasonably agree with each other, showing that the importance of the logarithms in the bottom quark mass is mild for what concerns the shape of the differential distributions. Their resummation indeed only affects the total rate, as shown in Fig. 2. However, the bin-by-bin NLO-to-LO ratio is far from being constant. Whereas in the case of pseudorapidity-ordered objects the shapes of the distributions are barely affected by the NLO corrections, the situation changes when the objects are p_T-ordered, so that NLO distributions are necessary for a precise determination of the observable.

In Fig. 4, we investigate other properties of single vector-like quark production, like the transverse momentum spectrum of the leading b-jet (left panel) that usually originates from the heavy quark decay, as well as the one of the leading muon (central panel) that is issued from the decay of the W-boson stemming from the heavy quark decay. As all particles can be seen as essentially massless compared with the mass scale of the heavy quark T, we

expect these two distributions to respectively peak around $M_T/2$ and $M_T/4$, as driven by the structure of the heavy quark decay,

$$T \to Wb \to \mu\nu_\mu b \,. \qquad (3.1)$$

The available energy is equally shared between the b-jet and the W-boson, such that both get a transverse momentum of $\mathcal{O}(M_T/2)$. The decay products of the W-boson are then expected to feature a p_T distribution peaking at about $M_T/4$. This property could be additionally illustrated by the missing transverse-momentum spectrum that would exhibit a similar structure as the muon p_T spectrum. The relevance of the NLO corrections can be seen especially in the tail of the leading b-jet p_T distribution, where the NLO distributions have a tendency to fall steeper with respect to their LO counterparts by virtue of the larger impact of the new channels for these phase space configurations.

In the right panel of the figure, we describe the hadronic activity typically associated with single vector-like quark production by presenting the H_T spectrum, where the H_T variable is defined as the scalar sum of the transverse momentum of all reconstructed jets of the event. The peak at about $M_T/2$ is due, once again, to the W-boson that carries away half of the available energy through its leptonic decay, and that is then not accounted for in the computation of the H_T variable. Also in this case the NLO distributions exhibit a steeper fall as a function of H_T, with respect to the LO ones. Nevertheless, the shape of the H_T observable may be impacted by contributions originating from higher orders. The bulk of the effect could however be derived by implementing the merging of multipartonic matrix elements featuring different jet multiplicities, both at LO and NLO. Such a study however lies beyond the scope of this work.

To summarize, in general we observe a substantial reduction of the uncertainties at NLO, and the 4FNS and 5FNS usually agreeing (in shape) with each other.

4. Conclusions

We have studied the phenomenology associated with the single production of a vector-like quark that couples to the third generation quarks of the Standard Model and to the weak gauge and Higgs bosons. We have estimated the impact of the NLO corrections in QCD, both in terms of the total production rate and of the differential distributions for the illustrative example of an up-type top partner. In the 4FNS, we have observed that the NLO-to-LO ratio of the total rate strongly depends on the vector-like quark mass, moving from values larger than 1 to values smaller than 1 when going from lower to higher masses. In the 5FNS, the same ratio is more stable, being always of the order of 0.95 in the whole mass range. Moreover, the shapes of the distributions are, to a large extent, independent of the way in which the bottom quark mass is treated and thus on the number of active quark flavours. We have also discussed in detail the features present in the distributions used for the experimental searches (both in the 4FNS and in the 5FNS) and in particular the role of the leading jets in these distributions. Regardless of the scheme used for the calculations, NLO corrections are mandatory for getting the theoretical uncertainties under control.

Our results therefore demonstrate that the inclusion of the NLO corrections in QCD are essential in order to properly study the single production of vector-like quarks at hadron colliders, like the LHC, and that the allowed different treatments of the bottom quark only affect the rates and the distributions in specific corners of the phase space.

References

[1] I. Antoniadis, A possible new dimension at a few TeV, Phys. Lett. B 246 (1990) 377–384.
[2] D.B. Kaplan, Flavor at SSC energies: a new mechanism for dynamically generated fermion masses, Nucl. Phys. B 365 (1991) 259–278.
[3] N. Arkani-Hamed, A.G. Cohen, E. Katz, A.E. Nelson, T. Gregoire, J.G. Wacker, The minimal moose for a little Higgs, J. High Energy Phys. 08 (2002) 021, arXiv: hep-ph/0206020 [hep-ph].
[4] R. Contino, L. Da Rold, A. Pomarol, Light custodians in natural composite Higgs models, Phys. Rev. D 75 (2007) 055014, arXiv:hep-ph/0612048 [hep-ph].
[5] O. Matsedonskyi, G. Panico, A. Wulzer, Light top partners for a light composite Higgs, J. High Energy Phys. 01 (2013) 164, arXiv:1204.6333 [hep-ph].
[6] ATLAS Collaboration, M. Aaboud, et al., Search for pair production of heavy vector-like quarks decaying to high-p_T W bosons and b quarks in the lepton-plus-jets final state in pp collisions at $\sqrt{s} = 13$ TeV with the ATLAS detector, J. High Energy Phys. 10 (2017) 141, arXiv:1707.03347 [hep-ex].
[7] ATLAS Collaboration, M. Aaboud, et al., Search for pair production of heavy vector-like quarks decaying into hadronic final states in pp collisions at $\sqrt{s} = 13$ TeV with the ATLAS detector, arXiv:1808.01771 [hep-ex].
[8] ATLAS Collaboration, M. Aaboud, et al., Combination of the searches for pair-produced vector-like partners of the third-generation quarks at $\sqrt{s} = 13$ TeV with the ATLAS detector, arXiv:1808.02343 [hep-ex].
[9] CMS Collaboration, A.M. Sirunyan, et al., Search for pair production of vector-like quarks in the bW$\overline{\text{b}}$W channel from proton-proton collisions at $\sqrt{s} = 13$ TeV, Phys. Lett. B 779 (2018) 82–106, arXiv:1710.01539 [hep-ex].
[10] CMS Collaboration, A.M. Sirunyan, et al., Search for vector-like T and B quark pairs in final states with leptons at $\sqrt{s} = 13$ TeV, J. High Energy Phys. 08 (2018) 177, arXiv:1805.04758 [hep-ex].
[11] J.A. Aguilar-Saavedra, D.E. López-Fogliani, C. Muñoz, Novel signatures for vector-like quarks, J. High Energy Phys. 06 (2017) 095, arXiv:1705.02526 [hep-ph].
[12] A. De Simone, O. Matsedonskyi, R. Rattazzi, A. Wulzer, A first top partner Hunter's guide, J. High Energy Phys. 04 (2013) 004, arXiv:1211.5663 [hep-ph].
[13] O. Matsedonskyi, G. Panico, A. Wulzer, On the interpretation of top partners searches, J. High Energy Phys. 12 (2014) 097, arXiv:1409.0100 [hep-ph].
[14] M. Backovic, T. Flacke, J.H. Kim, S.J. Lee, Search strategies for TeV scale fermionic top partners with charge 2/3, J. High Energy Phys. 04 (2016) 014, arXiv:1507.06568 [hep-ph].
[15] ATLAS Collaboration, M. Aaboud, et al., Search for pair production of up-type vector-like quarks and for four-top-quark events in final states with multiple b-jets with the ATLAS detector, J. High Energy Phys. 07 (2018) 089, arXiv:1803.09678 [hep-ex].
[16] ATLAS Collaboration, Search for Single Production of a Vector-Like B Quark Decaying into a Bottom Quark and a Higgs Boson which Decays into a Pair of Photons, Tech. Rep. ATLAS-CONF-2018-024, CERN, Geneva, Jul 2018, http://cds.cern.ch/record/2628759.
[17] CMS Collaboration, A.M. Sirunyan, et al., Search for single production of a vector-like T quark decaying to a Z boson and a top quark in proton-proton collisions at $\sqrt{s} = 13$ TeV, Phys. Lett. B 781 (2018) 574–600, arXiv:1708.01062 [hep-ex].
[18] CMS Collaboration, A.M. Sirunyan, et al., Search for single production of vector-like quarks decaying to a b quark and a Higgs boson, J. High Energy Phys. 06 (2018) 031, arXiv:1802.01486 [hep-ex].
[19] CMS Collaboration, A.M. Sirunyan, et al., Search for single production of vector-like quarks decaying to a top quark and a W boson in proton-proton collisions at $\sqrt{s} = 13$ TeV, arXiv:1809.08597 [hep-ex].
[20] J.M. Campbell, R. Frederix, F. Maltoni, F. Tramontano, NLO predictions for t-channel production of single top and fourth generation quarks at hadron colliders, J. High Energy Phys. 10 (2009) 042, arXiv:0907.3933 [hep-ph].
[21] B. Fuks, H.-S. Shao, QCD next-to-leading-order predictions matched to parton showers for vector-like quark models, Eur. Phys. J. C 77 (2) (2017) 135, arXiv:1610.04622 [hep-ph].
[22] M. Buchkremer, G. Cacciapaglia, A. Deandrea, L. Panizzi, Model independent framework for searches of top partners, Nucl. Phys. B 876 (2013) 376–417, arXiv:1305.4172 [hep-ph].

[23] A. Alloul, N.D. Christensen, C. Degrande, C. Duhr, B. Fuks, FeynRules 2.0 - a complete toolbox for tree-level phenomenology, Comput. Phys. Commun. 185 (2014) 2250–2300, arXiv:1310.1921 [hep-ph].

[24] C. Degrande, C. Duhr, B. Fuks, D. Grellscheid, O. Mattelaer, et al., UFO - the universal feynrules output, Comput. Phys. Commun. 183 (2012) 1201–1214, arXiv:1108.2040 [hep-ph].

[25] C. Degrande, Automatic evaluation of UV and R2 terms for beyond the standard model Lagrangians: a proof-of-principle, Comput. Phys. Commun. 197 (2015) 239–262, arXiv:1406.3030 [hep-ph].

[26] T. Hahn, Generating Feynman diagrams and amplitudes with FeynArts 3, Comput. Phys. Commun. 140 (2001) 418–431, arXiv:hep-ph/0012260 [hep-ph].

[27] G. Ossola, C.G. Papadopoulos, R. Pittau, On the rational terms of the one-loop amplitudes, J. High Energy Phys. 05 (2008) 004, arXiv:0802.1876 [hep-ph].

[28] J. Alwall, R. Frederix, S. Frixione, V. Hirschi, F. Maltoni, O. Mattelaer, H.S. Shao, T. Stelzer, P. Torrielli, M. Zaro, The automated computation of tree-level and next-to-leading order differential cross sections, and their matching to parton shower simulations, J. High Energy Phys. 07 (2014) 079, arXiv:1405.0301 [hep-ph].

[29] NNPDF Collaboration, R.D. Ball, et al., Parton distributions from high-precision collider data, Eur. Phys. J. C 77 (10) (2017) 663, arXiv:1706.00428 [hep-ph].

[30] A. Buckley, J. Ferrando, S. Lloyd, K. Nordström, B. Page, M. Rüfenacht, M. Schönherr, G. Watt, LHAPDF6: parton density access in the LHC precision era, Eur. Phys. J. C 75 (2015) 132, arXiv:1412.7420 [hep-ph].

[31] P. Artoisenet, R. Frederix, O. Mattelaer, R. Rietkerk, Automatic spin-entangled decays of heavy resonances in Monte Carlo simulations, J. High Energy Phys. 03 (2013) 015, arXiv:1212.3460 [hep-ph].

[32] T. Sjöstrand, S. Ask, J.R. Christiansen, R. Corke, N. Desai, P. Ilten, S. Mrenna, S. Prestel, C.O. Rasmussen, P.Z. Skands, An introduction to PYTHIA 8.2, Comput. Phys. Commun. 191 (2015) 159–177, arXiv:1410.3012 [hep-ph].

[33] E. Conte, B. Fuks, G. Serret, MadAnalysis 5, a user-friendly framework for collider phenomenology, Comput. Phys. Commun. 184 (2013) 222–256, arXiv:1206.1599 [hep-ph].

[34] E. Conte, B. Fuks, Confronting new physics theories to LHC data with MAD-ANALYSIS 5, Int. J. Mod. Phys. A 33 (28) (2018) 1830027, arXiv:1808.00480 [hep-ph].

[35] M. Cacciari, G.P. Salam, G. Soyez, The Anti-k(t) jet clustering algorithm, J. High Energy Phys. 04 (2008) 063, arXiv:0802.1189 [hep-ph].

[36] M. Cacciari, G.P. Salam, G. Soyez, FastJet user manual, Eur. Phys. J. C 72 (2012) 1896, arXiv:1111.6097 [hep-ph].

[37] G. Cacciapaglia, A. Deandrea, D. Harada, Y. Okada, Bounds and decays of new heavy vector-like top partners, J. High Energy Phys. 11 (2010) 159, arXiv:1007.2933 [hep-ph].

[38] F. Demartin, S. Forte, E. Mariani, J. Rojo, A. Vicini, The impact of PDF and alphas uncertainties on Higgs production in gluon fusion at hadron colliders, Phys. Rev. D 82 (2010) 014002, arXiv:1004.0962 [hep-ph].

[39] F. Maltoni, G. Ridolfi, M. Ubiali, b-Initiated processes at the LHC: a reappraisal, J. High Energy Phys. 1207 (2012) 022, arXiv:1203.6393 [hep-ph].

[40] J.A. Aguilar-Saavedra, R. Benbrik, S. Heinemeyer, M. Pérez-Victoria, Handbook of vectorlike quarks: mixing and single production, Phys. Rev. D 88 (9) (2013) 094010, arXiv:1306.0572 [hep-ph].